ELSEVIER

Journal of Organometallic Chemistry 643–644 (2002) 292–300

Journal of Organometallic Chemistry

www.elsevier.com/locate/jorganchem

Structural and electrochemical study of metal carbonyl complexes with chelating bis- and tetrakis(diphenylphosphino)tetrathiafulvalenes

Narcis Avarvari, David Martin, Marc Fourmigué *

'Sciences Moléculaires aux Interfaces', CNRS FRE 2068, Institut Jean Rouxel, 2, rue de la Houssinière, BP32229, 44322 Nantes Cedex 3, France

Received 10 July 2001; accepted 11 September 2001

Dedicated to Professor François Mathey on the occasion of his 60th birthday

Abstract

Several mono- and bimetallic complexes involving organometallic fragments such as $M(CO)_4$ (M = Mo, W), $Re(CO)_3Cl$ and $Fe(CO)_3$ coordinated to the chelating diphosphine 3,4-dimethyl-3′,4′-bis(diphenylphosphino)tetrathiafulvalene (**P2**) or tetraphosphine tetrakis(diphenylphosphino)tetrathiafulvalene (**P4**) have been synthesized and characterized. X-ray diffraction structures have been determined for **P4**$[W(CO)_4]_2$, **P2**$Re(CO)_3Cl$, **P2**$Fe(CO)_3$ and **P4**$[Fe(CO)_3]_2$. Octahedral geometries around the metallic center are observed for the tungsten and rhenium complexes, with a *fac* arrangement of the ligands for the latter, whereas slightly distorted trigonal bipyramid are found for both iron counter parts. Although the complexes are more difficult to oxidize than the corresponding free phosphines, as evidenced by cyclic voltammetry measurements, the first oxidation potentials remain in the usual range, thus offering the opportunity to generate stable radical cation salts. In the case of Fe complexes, the first oxidation wave corresponds to the formation of paramagnetic d^7 Fe(I) species, whereas in the Mo, W and Re complexes the metallic center is much more difficult to oxidize than the TTF core. © 2002 Elsevier Science B.V. All rights reserved.

Keywords: Tetrathiafulvalene; Phosphines; Metal carbonyl complexes; Crystal structures; Electrochemistry

1. Introduction

Chelating diphosphines such as bis(diphenylphosphino)methane (dppm) or bis(diphenylphosphino)-ethane (dppe) are well known for the stabilization of metal complexes in various oxidation states [1,2]. Their derivatization with redox active molecules such as ferrocene [3] or tetrathiafulvalene opens new routes toward the elaboration of hybrid molecules associating open-shell species of organic and inorganic character. Along these lines, several tetrathiafulvalenyl phosphines have already been described [4], either by functionalization of the TTF π-redox core by one, two or four diphenylphosphino moieties, as in 3,4-dimethyl-3′,4′-bis(diphenylphosphino)tetrathiafulvalene (hereafter **P2**) [5] or tetrakis(diphenylphosphino)tetrathiafulvalene (hereafter **P4**) [6], or by the insertion of a spacer between the PPh_2 and the TTF moieties [7].

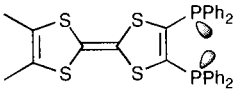

P2

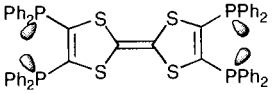

P4

In this paper, we investigate the coordination chemistry of these di- and tetraphosphines with Groups VI–VIII transition metal carbonyl fragments. The complexes of **P2** and **P4** with the organometallic fragments $Mo(CO)_4$, $W(CO)_4$, $Re(CO)_3Cl$ and $Fe(CO)_3$ will be described as well as their structural and electrochemical properties. Of specific interest are the relative redox potentials of these hybrid molecules where both the TTF π-redox core and the metal fragment are susceptible to oxidation to open-shell species.

* Corresponding author. Tel.: +33-240-373915; fax: +33-240-373995.

E-mail address: fourmigue@cnrs-imn.fr (M. Fourmigué).

0022-328X/02/$ - see front matter © 2002 Elsevier Science B.V. All rights reserved.
PII: S0022-328X(01)01249-9

2. Results and discussion

2.1. Synthesis and characterizations

The complexes were obtained in good yields as orange–red crystalline air-stable solids upon reaction of **P2** or **P4** with, respectively, one or two equivalents of the desired metallic precursors, i.e. *cis*-$[M(CO)_4(piperidine)_2]$ (M = Mo, W), $Re(CO)_5Cl$ and $Fe_2(CO)_9$ (Scheme 1). Both monometallic [**P2**][$Mo(CO)_4$] and [**P2**][$W(CO)_4$] complexes show the four absorptions characteristic of a tetracarbonyl unit with a *cis* arrangement of phosphines in the IR spectrum [8], while ^{31}P-NMR spectra display a singlet indicative of equivalent phosphorus environments. In all the complexes studied the phosphorus atoms resonate at lower field than the free phosphines in ^{31}P-NMR, which is a general tendency within this class of compounds [9]. In ^{13}C-NMR spectrum of [**P2**][$W(CO)_4$], we can clearly observe the resonance of two different types of CO, the axial and the equatorial ones, with the corresponding coupling constants. This observation proves the rigidity in solution of the coordination sphere of the tungsten center. The corresponding [**P2**][$Re(CO)_3Cl$] complex exhibits three absorption bands in the carbonyl region, a signature of a *fac* isomer while only two bands are usually encountered with the *mer* isomer [10]. This stereochemistry is further substantiated by the presence of a single peak in the ^{31}P-NMR spectrum and by its X-ray crystal structure (see below). Similarly, the iron complex [**P2**][$Fe(CO)_3$] exhibits, as expected, an unique resonance in ^{31}P-NMR. The carbonyl carbon atoms resonate as a triplet in ^{13}C-NMR, thus proving their equivalence in solution, at the NMR time scale. The flexibility of the coordination sphere around a pentacoordinated iron center is a well-known phenomenon [11] relying on the easy interconversion between a trigonal bipyramidal geometry and a square planar pyramidal one. Infrared spectrum shows the three characteristic bands of a $L_2Fe(CO)_3$ complex type, where L_2 is a chelating ligand [12]. A single crystal X-ray measurement, discussed below, definitely proved the structure of the complex in solid state.

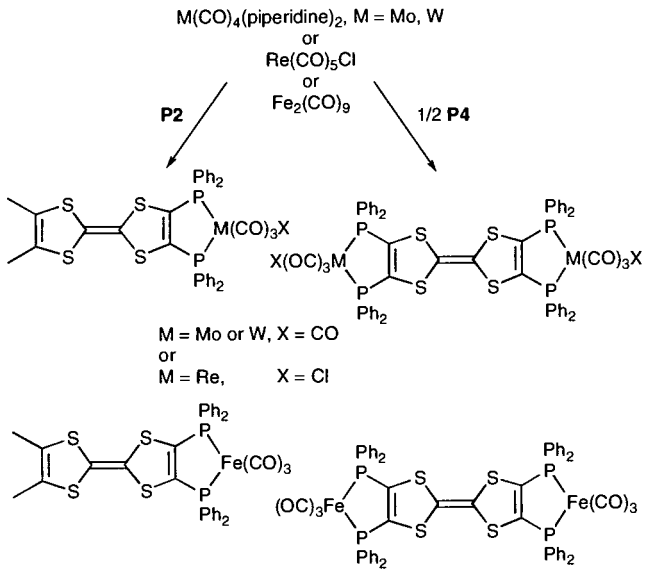

Scheme 1.

Table 1
Selected bond lengths and bond angles in [**P4**][$W(CO)_4$]$_2$[toluene]$_3$

Bond lengths			
W(1)–P(1)	2.4872(8)	W(1)–C(4)	1.988(3)
W(1)–P(2)	2.4749(7)	C(1)–O(1)	1.153(4)
W(1)–C(1)	1.993(3)	C(2)–O(2)	1.141(4)
W(1)–C(2)	2.033(3)	C(3)–O(3)	1.145(4)
W(1)–C(3)	2.023(3)	C(4)–O(4)	1.151(4)
Bond angles			
P(1)–W(1)–P(2)	79.97(2)		

As their **P2** counter parts, the bimetallic complexes [**P4**][$Mo(CO)_4$]$_2$ and [**P4**][$W(CO)_4$]$_2$ show also the four IR absorptions characteristic of a tetracarbonyl unit with a *cis* arrangement of phosphines and wavelengths very close to those of the corresponding monometallic complexes. The bimetallic complex [**P4**][$W(CO)_4$]$_2$ was also characterized by X-ray diffraction. On the other hand, four bands were observed in the IR spectrum of [**P4**][$Re(CO)_3Cl$]$_2$. Together with the observation of two peaks in ^{31}P-NMR (see Section 4), these results indicate that two diastereoisomers were formed simultaneously in the case of this bimetallic complex. This is not surprising, since one can expect the chlorine ligands to adopt both *cis* and *trans* positions relative to the TTF plane in a bis(*fac*) arrangement around the two metallic centers. On the other hand, the bimetallic iron complex [**P4**][$Fe(CO)_3$]$_2$ presents only one isomer in solution, as attested by ^{31}P- and ^{13}C-NMR spectra. The infrared spectrum, measured in KBr, shows three absorption bands, as in the **P2** counter part. An X-ray diffraction experiment allowed us to characterize the bimetallic complex in solid state.

2.2. X-ray structures

[**P4**][$W(CO)_4$]$_2$ crystallizes as a toluene solvate in the monoclinic system, space group $P2_1/c$, with one molecule located on the inversion center, one toluene molecule disordered on an inversion center and one toluene molecule in general position in the unit cell. Bond lengths within the coordination sphere of the W atom (Table 1) are in the usual range as are the bond lengths within the TTF core. An ORTEP view with partial numbering scheme is given in Fig. 1. The metal–carbon bonds *trans* to phosphorus are slightly shorter than those of *cis*, the average difference being 0.038 Å. The dithiole rings are not folded along the S···S hinge

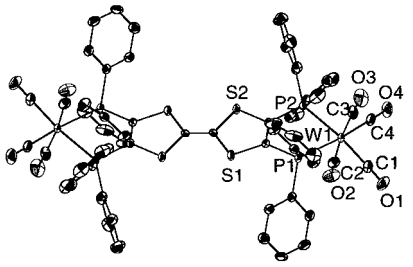

Fig. 1. ORTEP view of the bimetallic complex [**P4**][$W(CO)_4$]$_2$.

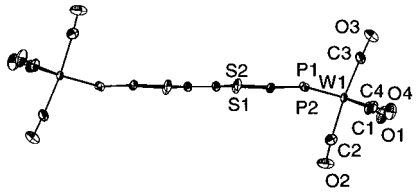

Fig. 2. Side view of [**P4**][$W(CO)_4$]$_2$ showing the folding of the metallacycle along the P···P hinge.

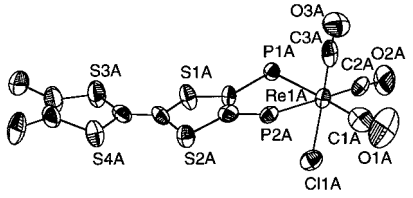

Fig. 3. ORTEP view of [**P2**][$Re(CO)_3Cl$]. The phenyl rings have been omitted for clarity.

Table 2
Selected bond distances and bond angles in [**P2**][$Re(CO)_3Cl$][toluene]

Bond lengths			
Re(1A)–P(1A)	2.459(4)	Re(1B)–P(1B)	2.451(4)
Re(1A)–P(2A)	2.455(4)	Re(1B)–P(2B)	2.447(4)
Re(1A)–Cl(1A)	2.502(4)	Re(1B)–Cl(1B)	2.492(4)
Re(1A)–C(1A)	1.93(2)	Re(1B)–C(1B)	1.97(2)
Re(1A)–C(2A)	1.89(2)	Re(1B)–C(2B)	1.89(2)
Re(1A)–C(3A)	1.80(2)	Re(1B)–C(3B)	1.83(2)
C(1A)–O(1A)	1.12(2)	C(1B)–O(1B)	1.16(2)
C(2A)–O(2A)	1.21(2)	C(2B)–O(2B)	1.21(2)
C(3A)–O(3A)	1.21(2)	C(3B)–O(3B)	1.21(2)
Bond angles			
P(1A)–Re(1A)–P(2A)	80.89(12)	P(1B)–Re(1B)–P(2B)	81.00(12)

while the metallacycles C_2P_2W are folded by 17.37(8)°, as already observed in the few $W(CO)_4$ complexes with conjugated chelating diphosphines such as the tetrakis-(diphenylphosphino)benzene-bis(tetracarbonyltungsten) complex [13]. In Fig. 2 we present a side view of the molecule, allowing the easy observation of this distortion. A similar folding (15–17°) is also found in the corresponding molybdenum complex [13] as well as in monometallic complexes with 1,2-bis(diphenylphosphino)ethylene [14] or 1,2-bis(diphenylphosphino)-propene [15].

[**P2**][$Re(CO)_3Cl$] crystallizes in the orthorhombic system, space group $Pna2_1$, with two crystallographically independent and two toluene molecules in the unit cell (Fig. 3). Both molecules are almost identical and appear to correspond to each other through a pseudo-inversion center while the toluene molecules do not. Bond lengths and angles in the coordination sphere of the Re atom are collected in Table 2. The structure reveals a *facial* arrangement for the carbonyl groups consistent with the structural assignment from IR studies [16]. The metallacycle is folded by 23.2(4)° along the P···P hinge while the TTF core is also affected since the dithiole ring bearing the two diphenylphosphino groups is folded by 24(1)° along the S···S hinge. This folding of the dithiole ring has been often observed in several **P2** and **P4** complexes [6,17] and illustrates the flexibility of the TTF core.

Suitable X-ray diffraction crystals of [**P2**][$Fe(CO)_3$] were obtained by recrystallization in hexane. The structure was solved in the orthorhombic system, space group *Pbca*, with two crystallographically independent molecules and one molecule of hexane located on an inversion center. Thus, the complex crystallized as a solvate with one molecule of hexane to four molecules of complex. The solvent is located in the structure between the planes defined by the donors. No short intermolecular van der Waals S···S contacts are observed within these planes. Bond lengths and angles in the coordination sphere of Fe are listed in Table 3. An ORTEP representation of one (Fe1) of the two independent molecules of complex is shown in Fig. 4. The coordination geometry around the metallic center is of distorted trigonal bipyramid (tbp) type, with the diphosphine occupying one axial and one equatorial

Table 3
Selected bond distances and bond angles in [**P2**][$Fe(CO)_3$][hexane]$_{1/4}$

Bond lengths			
Fe(1)–C(33)	1.757(6)	Fe(2)–C(68)	1.749(6)
Fe(1)–C(34)	1.752(6)	Fe(2)–C(69)	1.737(6)
Fe(1)–C(35)	1.756(5)	Fe(2)–C(70)	1.746(6)
Fe(1)–P(1)	2.213(1)	Fe(2)–P(3)	2.195(1)
Fe(1)–P(2)	2.184(1)	Fe(2)–P(4)	2.215(1)
C(33)–O(1)	1.158(5)	C(68)–O(4)	1.153(6)
C(34)–O(2)	1.158(5)	C(69)–O(5)	1.161(5)
C(35)–O(3)	1.145(4)	C(70)–O(6)	1.154(5)
Bond angles			
C(33)–Fe(1)–C(34)	122.3(2)	C(68)–Fe(2)–C(69)	89.3(3)
C(33)–Fe(1)–C(35)	93.6(2)	C(68)–Fe(2)–C(70)	95.6(3)
C(34)–Fe(1)–C(35)	90.0(2)	C(69)–Fe(2)–C(70)	115.2(2)
C(33)–Fe(1)–P(1)	91.71(15)	C(68)–Fe(2)–P(3)	85.01(17)
C(34)–Fe(1)–P(1)	89.06(15)	C(69)–Fe(2)–P(3)	130.90(18)
C(35)–Fe(1)–P(1)	174.29(16)	C(70)–Fe(2)–P(3)	113.86(18)
C(33)–Fe(1)–P(2)	106.21(16)	C(68)–Fe(2)–P(4)	170.37(17)
C(34)–Fe(1)–P(2)	131.36(18)	C(69)–Fe(2)–P(4)	94.15(19)
C(35)–Fe(1)–P(2)	90.08(16)	C(70)–Fe(2)–P(4)	91.06(17)
P(1)–Fe(1)–P(2)	86.32(4)	P(3)–Fe(2)–P(4)	85.95(4)

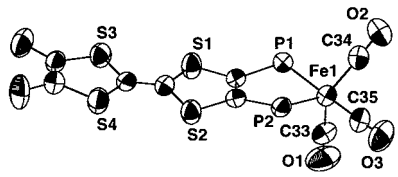

Fig. 4. ORTEP view of [**P2**][$Fe(CO)_3$]. The phenyl rings have been omitted for clarity.

Table 4
Selected bond distances and bond angles in [**P4**][$Fe(CO)_3$]$_2$

Bond lengths			
Fe–C(28)	1.771(3)	Fe–P(2)	2.214(1)
Fe–C(29)	1.775(4)	C(28)–O(1)	1.140(3)
Fe–C(30)	1.773(4)	C(29)–O(2)	1.153(4)
Fe–P(1)	2.193(1)	C(30)–O(3)	1.153(4)
Bond angles			
C(28)–Fe–C(29)	91.01(15)	C(30)–Fe–P(1)	120.83(11)
C(28)–Fe–C(30)	91.46(14)	C(28)–Fe–P(2)	175.58(9)
C(29)–Fe–C(30)	119.77(15)	C(29)–Fe–P(2)	90.25(10)
C(28)–Fe–P(1)	88.95(10)	C(30)–Fe–P(2)	91.59(9)
C(29)–Fe–P(1)	119.39(11)	P(1)–Fe–P(2)	86.74(4)

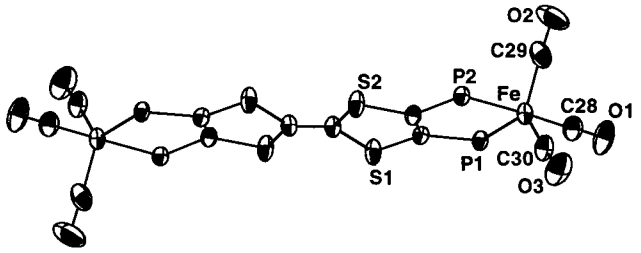

Fig. 5. ORTEP view of the bimetallic complex [**P4**][$Fe(CO)_3$]$_2$. The phenyl rings have been omitted for clarity.

site. This situation is usually encountered within other unsaturated *cis* diphosphine $Fe(CO)_3$ complexes [18]. In order to distinguish between the two possible limit cases of a pentacoordinated iron center, one can simply apply the τ test [19], where $\tau = (\alpha - \beta)/60$. The parameters α and β represent the largest angle and second largest angle, respectively, around the metallic center. The value of τ ranges from 0, for a perfect square pyramid, to 1 for a trigonal bipyramid. In our case $\tau(Fe1) = 0.72$ and $\tau(Fe2) = 0.66$, hence the ligands around Fe define a distorted trigonal bipyramid geometry. A τ value of the same order of magnitude (0.76) was observed for [$C_2H_2(PPh_2)_2$][$Fe(CO)_3$] [18c], whereas in the saturated counter part, (dppe)$Fe(CO)_3$ ($\tau = 0.35$), the iron center is clearly in a distorted square pyramidal environment. Another interesting point concerning our complex is, as in the case of the rhenium complex discussed above, the distortions from the planarity within the dithiole moiety bearing the phosphine groups, along S···S and P···P axes. The first one, with folding angles of 9.3(2)° for S1···S2 (Fe1) and 13.5(2)° for S5···S6 (Fe2), shows the influence of the complexation on the TTF core. A much larger difference between the two independent molecules Fe1 and Fe2 can be observed when taking into account the second distortion. Indeed, values of 21.1(1)° (Fe1) and 10.2(1)° (Fe2) for the folding angles along the P···P hinge support this difference and suggest a certain flexibility of the five-membered ring metallacycle. Finally we note that the axial Fe–P bonds are slightly longer than the equatorial ones by 0.03 Å (Fe1) and 0.02 Å (Fe2), likely because of the weaker π-retrodonation due to the axial CO. All the other structural parameters are in the usual range and deserve no special comments.

In the case of bimetallic [**P4**][$Fe(CO)_3$]$_2$ we could obtain suitable X-ray diffraction crystals by recrystallization in acetonitrile or in toluene. We discuss hereafter only the structure of the complex recrystallized in acetonitrile, whose quality is somewhat better than the other one, in which disordered molecules of toluene are present. Thus, the complex crystallizes in the triclinic system, space group $P\bar{1}$, with one independent molecule located on the inversion center. Bond lengths and angles, among which those concerning the coordination sphere of Fe are listed in Table 4, are in the usual range. An ORTEP view of the molecular structure is presented in Fig. 5. The TTF core is slightly distorted, the folding angle along the S···S axis being 5.9(3)°. A drastic decrease, down to 2.0(1)°, is observed for the folding angle about the P···P axis, when comparing with the monometallic complex described above. This leads to an almost planar five-membered ring metallacycle. The coordination geometry around the iron center is almost a perfect trigonal bipyramid, since τ amounts 0.91 (see above), with an axial and an equatorial phosphine. On the contrary, in the bimetallic complex tetrakis(diphenylphosphino)benzene-bis(tricarbonyliron) [20], the geometry at Fe is intermediate between trigonal bipyramidal and square pyramidal ($\tau = 0.50$).

2.3. Electrochemistry

Cyclic voltammetry data for all the complexes along with those already published [6] for **P2** and **P4** are given in Table 5. As a general remark, the donors experience, especially for the first oxidation wave, a strong anodic shift upon complexation comparing with the free phosphines oxidation potentials. This means that significant through space or through bond interactions between the TTF core and the metallic fragment occur. Nevertheless, these potentials are still below 1 V and open the possibility of synthesizing, by electrocrystallization, air-stable open-shell species bearing organometallic fragments.

In Fig. 6, we have represented the cyclic voltammetry curves for both mono- and bimetallic tungsten com-

plexes. The molybdenum complexes show similar curves. Two reversible one-electron TTF based redox processes are observed for the monometallic $\mathbf{P_2}W$ and $\mathbf{P_2}Mo$ complexes. Anodic shifts of 220 and 200 mV, respectively, are noticed for the first oxidation potential, whereas the second one is less influenced by the metallic fragment. A third oxidation weakly reversible wave at about $E_{ox} = +1.25$ V is observed. A better reversibility is obtained at higher scan rates. This process was assigned to an one-electron oxidation of the metallic center, which is likely to be decomposed by loss of carbonyl ligands upon oxidation. Electrochemical studies [21] dealing with [*cis*-$P_2M(CO)_4$] (M = Mo or W) type complexes show that an irreversible one-electron oxidation of the metal occurs at potentials around +1.1 V and, accordingly, the instability of the oxidized species relies on the fast dissociation of the carbonyl ligands. In the case of bimetallic $\mathbf{P_4}W_2$ and $\mathbf{P_4}Mo_2$ only the reversible wave corresponding to the monoelectronic oxidation of TTF core in radical cation is observed, with a strong anodic shift of 400 and 380 mV, respectively, versus free **P4**, which means a roughly double influence upon complexation than in the case of monometallic counter parts. Subsequently, the oxidation of TTF^{+} to TTF^{2+} and that of M^0 to M^{+1} probably occurs at very close potentials, hence only a broad irreversible oxidation wave is observed at about +1.28 V.

Table 5
Cyclic voltammetry data

Compound	$E1_M$ (ΔE)	$E1_{TTF}$ (ΔE)	$E2_{TTF}$ (ΔE)	$E1_{M'}$
P2 [a]		0.27; r	0.81; r	
P4 [a]		0.33; r	0.73; r	
[**P2**][$Fe(CO)_3$] [a]	0.28 (112); r	0.68 (183); r	1.18 (165); r	
[**P4**][$Fe(CO)_3]_2$ [a]	0.31 (80); r	1.04; wr		
[**P2**][$Mo(CO)_4$] [b]		0.47 (60); r	0.85 (60); r	1.25; wr
[**P4**][$Mo(CO)_4]_2$ [a]		0.71 (68); r	1.23; ir	
[**P2**][$W(CO)_4$] [b]		0.49 (60); r	0.86 (64); qr	1.26; wr
[**P4**][$W(CO)_4]_2$ [a]		0.73 (64); r	1.33; ir	
[**P2**][$Re(CO)_3Cl$] [b]		0.52 (59); r	0.90 (59); r	1.64; ir
[**P4**][$Re(CO)_3Cl]_2$ [b]		0.82 (60); r	1.15 (59); r	1.64; ir

Potentials are expressed in V vs. SCE and ΔE in mV. For the reversible (r) and quasi-reversible (qr) processes the half-wave potentials ($E_{1/2}$) are given, whereas only the oxidation potentials (E_{ox}) are shown for the weak-reversible (wr) and irreversible (ir) processes. The free phosphines oxidation potentials were taken from Ref. [6]. $E1_M$ and $E1_{M'}$ refer to metal centered redox processes, whereas $E1_{TTF}$ and $E2_{TTF}$ are related to the TTF framework.

[a] CH_2Cl_2, *n*-Bu_4NPF_6, 0.05 M, 100 mV s^{-1}.

[b] CH_3CN, *n*-Bu_4NPF_6, 0.05 M, 100 mV s^{-1}.

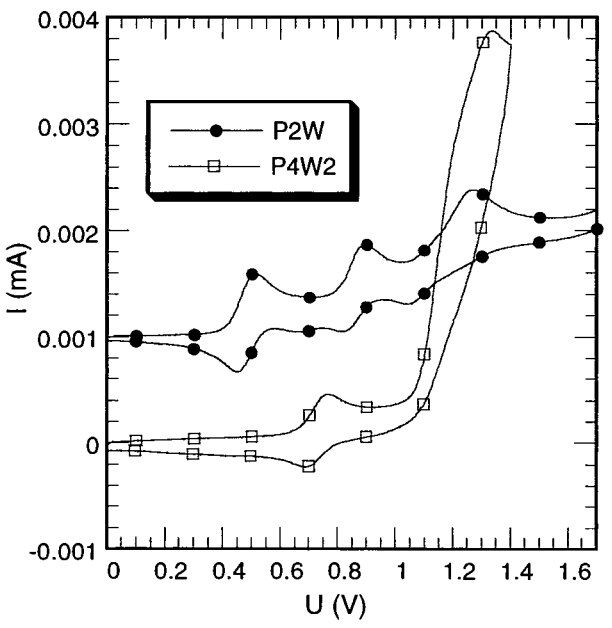

Fig. 6. Cyclic voltammetry curves for [**P2**][$W(CO)_4$] and [**P4**][$W(CO)_4]_2$.

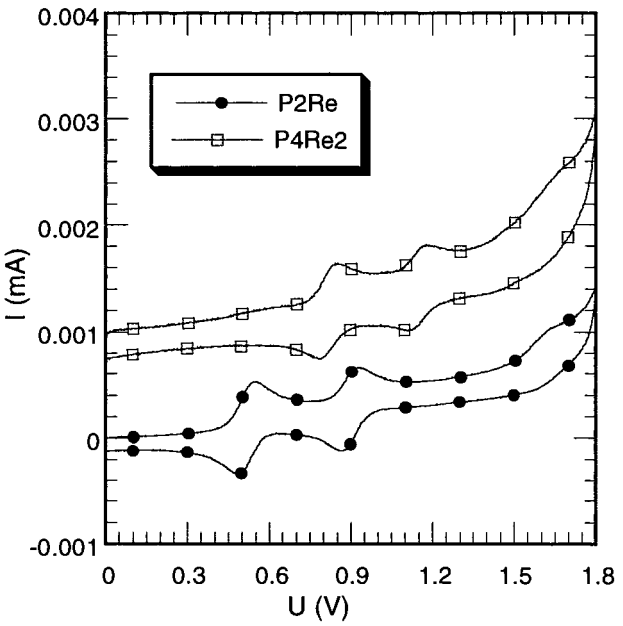

Fig. 7. Cyclic voltammetry curves for [**P2**][$Re(CO)_3Cl$] and [**P4**][$Re(CO)_3Cl]_2$.

The cyclic voltammetry curves corresponding to the rhenium complexes are shown in Fig. 7. Two reversible one-electron TTF based redox processes are observed for both monometallic and bimetallic complexes. Larger anodic shifts than in the case of Group VI metal complexes discussed above characterize both Re complexes versus the free ligands. This is not surprising, since an electron poorer metallic fragment is coordinated to the same TTF framework. Re(I) centers in such a kind of environment are known to be hard to oxidize. Reports in the literature [10a,16] mention that the irreversible oxidation of *fac*-$P_2XRe(CO)_3$ complexes arises at potentials around +1.4–1.6 V. This is in good agreement with our curves, where a broad peak at

+1.64 V can be observed. Thus, if taking into account the stability of these organo-rhenium fragments toward oxidation, our complexes are potential good candidates for electrocrystallization experiments where the metallic center plays basically a structural role.

A very different electrochemical behavior, when compared with the cases discussed above, is displayed by the $\mathbf{P_2}Fe$ and $\mathbf{P_4}Fe_2$ complexes. It is well established [22] that $P_2Fe(CO)_3$ complexes are readily oxidized in non-coordinating solvents, such CH_2Cl_2, in a reversible one-electron process to lead at a paramagnetic 17-electron species. The oxidation potentials range from 0.12 V when P_2 = dppe to 0.69 V for $P_2 = [P(OPh)_3]_2$, with a peak separation ΔE of about 150–170 mV, and the paramagnetic complexes have been evidenced by EPR and IR measurements. A more exhaustive crystallographic, EPR and theoretical study [23] dealing with $[(PPh_3)_2Fe(CO)_3]^+$ complex shows that the iron center adopts a square pyramidal geometry in solution as well as in solid state, with the unpaired electron located in the $Fe(d_{z^2})$ orbital. Thus, the possibility to have paramagnetic metallic centers in the vicinity of an organic TTF based radical, within the $\mathbf{P_2}Fe$ and $\mathbf{P_4}Fe_2$ complexes, appeared to us particularly interesting. The cyclic voltammetry curves represented in Fig. 8 show, as expected, a first reversible oxidation wave for both complexes, relying on the generation of paramagnetic d^7 iron species. The corresponding potential values, listed in Table 5, are in the usual range. In the case of bimetallic $\mathbf{P_4}Fe_2$ a concomitant one-electron oxidation of both Fe centers is likely to occur, since no splitting, even at very low scan rate, was observed for this wave.

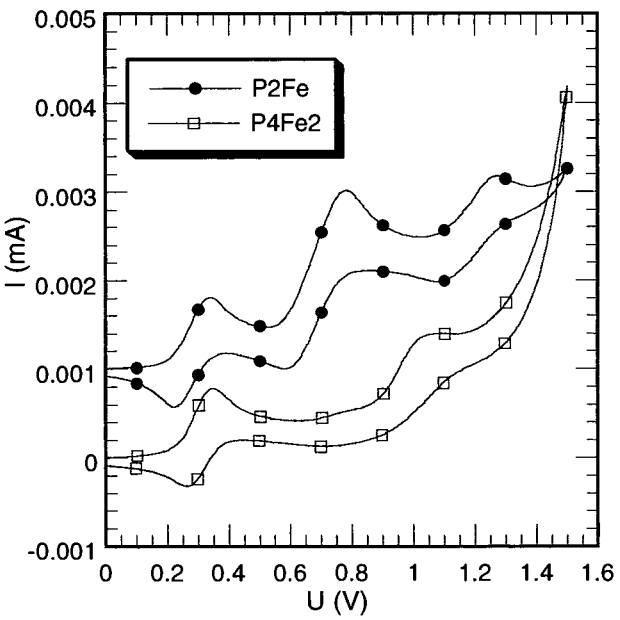

Fig. 8. Cyclic voltammetry curves for [**P2**][$Fe(CO)_3$] and [**P4**][$Fe(CO)_3$]$_2$.

A much weaker reversibility for this redox process, hence lower stability for the paramagnetic 17-electron species, is observed when the cyclic voltammetry measure is performed in acetonitrile, certainly because of a fast ligand exchange. Subsequently, the oxidation of the TTF core in $\mathbf{P_4}Fe_2$ appears to be quite difficult and only weakly reversible. Conversely, more encouraging electrochemical data are obtained for the monometallic complex, since two reversible TTF based oxidation steps are observed after the first metal based oxidation wave generating a positive charged species. Therefore it is not surprising to note a much larger anodic shift versus free **P2**, than those observed for the Mo, W and Re counter parts, for the one-electron oxidation of TTF core in radical cation. However, a potential value of +0.68 V remains in the usual range of TTF donors, thus the obtention of mixed organic–organometallic diradical species can be envisaged.

3. Conclusions

The new synthesized organometallic TTF based complexes appear to be interesting electro-active molecular precursors. The organometallic fragments could either play mainly a structural role (M = Mo, W, Re) or be directly involved in the redox processes, thus competing with the TTF core (M = Fe). Further work will be devoted to the obtention, by electrocrystallization experiments, of radical cation salts derived from these precursors.

4. Experimental

4.1. General

P2 and **P4** were prepared by published procedures [5,6]. $Re(CO)_5Cl$ and $Fe_2(CO)_9$ were obtained from Strem Chemicals and used as received. *cis*-$Mo(CO)_4(piperidine)_2$ and *cis*-$W(CO)_4(piperidine)_2$ were prepared from $Mo(CO)_6$ and $W(CO)_6$ as described elsewhere [24]. Dry toluene was obtained by distillation from Na and dry CH_2Cl_2 by distillation from P_2O_5. Nuclear magnetic resonance spectra were recorded in a Bruker ARX 400 spectrometer operating at 400.13 MHz for ^1H, 100.62 MHz for ^{13}C and 161.97 MHz for ^{31}P. Chemical shifts are expressed in parts per million downfield from external Me_4Si (^1H and ^{13}C) and 85% H_3PO_4 (^{31}P). Coupling constants J are expressed in Hz. The following abbreviations are used: s, singlet; d, doublet, t, triplet, m, multiplet, b, broad, v, virtual. Mass spectra were performed in a HP 5989A spectrometer in the EI mode, with an ionization energy of 70 eV. Infrared spectra were measured in a FTIR Nicolet 20 SXC spectrometer. Elemental analyses were performed

by the 'Service d'Analyse du CNRS', at Gif-sur-Yvette, France. Cyclic voltammetry experiments were performed in a VPM potentiostat in dried CH_3CN or CH_2Cl_2 solutions of 0.05 M n-Bu_4NPF_6 as electrolyte at room temperature (r.t.). A negligible difference of about 10 mV was noticed between the potential values measured in CH_3CN and in CH_2Cl_2. A Pt working electrode (diameter 1 mm), a Pt counter electrode and a SCE reference electrode were used.

4.2. Synthesis and characterization of complexes

4.2.1. [3,4-Bis(diphenylphosphino)-3′,4′-dimethyltetrathiafulvalene]rheniumtricarbonyl-chloride, [P2][Re(CO)$_3$Cl]

P2 (300 mg, 0.5 mmol) in dry toluene (50 ml) and $Re(CO)_5Cl$ (180 mg, 0.5 mmol) were heated under reflux for 2 days. After cooling at 0 °C, the orange microcrystals were filtered and recrystallized from toluene to afford [**P2**][$Re(CO)_3Cl$] as orange crystals (339 mg, 75%). Anal. Calc. for $C_{35}H_{26}ClP_2O_3Re{\cdot}C_7H_8$: C, 50.52; H, 3.43; P, 6.20; S, 12.84. Found: C, 50.08; H, 3.37; P, 7.29; S, 12.81%. IR (KBr, cm^{-1}): ν_{CO} 1916, 1949, 2028. ^{31}P-NMR ($CDCl_3$): δ 22.9. ^{1}H-NMR ($CDCl_3$): δ 7.35–7.51 (m, 12H, H_{meta}, H_{para}), 7.71–7.85 (m, 8H, H_{ortho}).

4.2.2. Tetrakis(diphenylphosphino)tetrathiafulvalenebis-[rheniumtricarbonylchloride)], [P4][Re(CO)$_3$Cl]$_2$

P4 (280 mg, 0.3 mmol) and $Re(CO)_5Cl$ (310 mg, 0.8 mmol) were heated under reflux in toluene (50 ml) for 4 h. Cooling the solution at −18 °C afforded a microcrystalline orange solid (205 mg, 44%) representing a mixture of two diasteroisomers in a ratio A/B of 1:1.6, according to ^{31}P-NMR spectrum. Anal. Calc. for $C_{60}H_{40}Cl_2O_6P_4S_4Re_2$: C, 46.42; H, 2.60; Cl, 4.57. Found: C, 45.69; H, 2.52; Cl, 5.82%. IR (KBr, cm^{-1}): ν_{CO} 1905, 1931, 1974, 2033. ^{31}P-NMR (CD_2Cl_2): δ 23.5 (B), 24.6 (A). ^{1}H-NMR (CD_2Cl_2): δ 7.37–7.53 (m, 24H, H_{meta}, H_{para}), 7.77–7.91 (m, 16H, H_{ortho}).

4.2.3. [3,4-Bis(diphenylphosphino)-3′,4′-dimethyltetrathiafulvalene][tetracarbonyl)]molybdenum, [P2][Mo(CO)$_4$)]

$Mo(CO)_4$(piperidine)$_2$ (120 mg, 0.32 mmol) and **P2** (200 mg, 0.33 mmol) were dissolved in CH_2Cl_2 (30 ml) and the solution heated to reflux for 1.5 h. The orange solution turned dark red. After concentration and layering with MeOH, dark red crystals of [**P2**][$Mo(CO)_4$)] were obtained (175 mg, 64%). Anal. Calc. for $C_{36}H_{26}O_4P_2S_4Mo$: C, 53.46; H, 3.24; S, 15.86. Found: C, 53.27; H, 3.13; S, 16.17%. IR (KBr, cm^{-1}): ν_{CO} 1891, 1908, 1934, 2024. ^{31}P-NMR ($CDCl_3$): δ 51.9. ^{1}H-NMR (CD_2Cl_2): δ 7.42 (bs, 12H, H_{meta}, H_{para}), 7.51–7.59 (m, 8H, H_{ortho}).

4.2.4. [Tetrakis(diphenylphosphino)tetrathiafulvalene]-bis[tetracarbonyl(molybdenum)], [P4][Mo(CO)$_4$]$_2$

$Mo(CO)_4$(piperidine)$_2$ (250 mg, 0.66 mmol) and **P4** (200 mg, 0.21 mmol) were dissolved in CH_2Cl_2 (30 ml) and heated to reflux for 2.5 h. After cooling and MeOH addition, the precipitated violet solid was filtered and recrystallized from toluene to afford [**P4**][$Mo(CO)_4$]$_2$ as violet crystals (214 mg, 74%). Anal. Calc. for $C_{62}H_{40}O_8P_4S_4Mo_2{\cdot}(C_7H_8)_3$: C, 61.03; H, 3.95; P, 7.58; S, 7.85. Found: C, 61.17; H, 3.97; P, 7.52; S, 7.67%. IR (KBr, cm^{-1}): ν_{CO} 1884, 1911, 1932, 2023. ^{31}P-NMR ($CDCl_3$): δ 52.8. ^{1}H-NMR (CD_2Cl_2): δ 7.48 (bs, 24H, H_{meta}, H_{para}), 7.50–7.58 (m, 16H, H_{ortho}).

4.2.5. [3,4-Bis(diphenylphosphino)-3′,4′-dimethyltetrathiafulvalene][tetracarbonyl]tungsten, [P2][W(CO)$_4$]

$W(CO)_4$(piperidine)$_2$ (152 mg, 0.33 mmol) and **P2** (200 mg, 0.33 mmol) were dissolved in CH_2Cl_2 (25 ml) and the solution warmed to reflux for 2.5 h. After cooling and slow MeOH diffusion, violet crystals were filtered (232 mg, 78%). Anal. Calc. for $C_{32}H_{26}P_2O_4S_4W$: C, 48.22; H, 2.92; S, 14.30. Found: C, 48.26; H, 2.90; S, 13.23%. IR (KBr, cm^{-1}): ν_{CO} 1879, 1901, 1920, 2021. ^{31}P-NMR ($CDCl_3$): δ 35.0 ($^1J_{P^{183}W} = 238.6$ Hz). ^{1}H-NMR (CD_2Cl_2): δ 7.40 (bs, 12H, H_{meta}, H_{para}), 7.49–7.57 (m, 8H, H_{ortho}). ^{13}C-NMR (CD_2Cl_2): δ 13.5 (s, CH_3), 114.3 (s, $S_2C{=}CS_2$), 114.6 (s, $S_2C{=}CS_2$), 123.3 (s, $CH_3C{=}$), 129.2 (d, $^3J_{CP} = 10.1$ Hz, C_{meta}), 131.1 (s, C_{para}), 132.6 (d, $^2J_{CP} = 13.0$ Hz, C_{ortho}), 134.4 (dd, $^1J_{CP} = 42.6$ Hz, $^4J_{CP} = 2.2$ Hz, C_{ipso}), 152.5 (dd, $^1J_{CP} = 39.5$ Hz, $^2J_{CP} = 20.2$ Hz, PC=CP), 201.0 (t, $^2J_{CP} = 6.4$ Hz, CO_{ax}), 206.5 (dd, $^2J_{CP(trans)} = 25.7$ Hz, $^2J_{CP(cis)} = 5.9$ Hz, CO_{eq}).

4.2.6. [Tetrakis(diphenylphosphino)tetrathiafulvalene]-bis[tetracarbonyl(tungsten)], [P4][W(CO)$_4$]$_2$

A solution of $W(CO)_4$(piperidine)$_2$ (200 mg, 0.43 mmol) and **P4** (200 mg, 0.21 mmol) in CH_2Cl_2 is heated under reflux for 2.5 h. The product is precipitated by addition of MeOH, filtered and recrystallized from toluene to afford burgundy red crystal (205 mg, 53%). Anal. Calc. for $C_{62}H_{40}O_8P_4S_4W_2{\cdot}(C_7H_8)_3$: C, 55.10; H, 3.57; S, 7.09. Found: C, 55.17; H, 3.59; S, 9.69%. IR (KBr, cm^{-1}): ν_{CO} 1877, 1903, 1925, 2019. ^{31}P-NMR (CD_2Cl_2): δ 35.9 ($^1J_{P^{183}W} = 238.4$ Hz). ^{1}H-NMR (CD_2Cl_2): δ 7.43 (bs, 24H, H_{meta}, H_{para}), 7.48–7.55 (m, 16H, H_{ortho}). ^{13}C-NMR (CD_2Cl_2): δ 119.2 (s, $S_2C{=}CS_2$), 129.1 (d, $^3J_{CP} = 10.2$ Hz, C_{meta}), 131.2 (s, C_{para}), 132.5 (d, $^2J_{CP} = 13.1$ Hz, C_{ortho}), 134.5 (dd, $^1J_{CP} = 42.8$ Hz, $^4J_{CP} = 2.1$ Hz, C_{ipso}), 152.3 (dd, $^1J_{CP} = 39.4$ Hz, $^2J_{CP} = 20.3$ Hz, PC=CP), 201.1 (t, $^2J_{CP} = 6.5$ Hz, CO_{ax}), 206.7 (dd, $^2J_{CP(trans)} = 25.5$ Hz, $^2J_{CP(cis)} = 5.8$ Hz, CO_{eq}).

4.2.7. [3,4-Bis(diphenylphosphino)-3′,4′-dimethyltetrathiafulvalene][tricarbonyl]iron, [P2][Fe(CO)$_3$]

P2 (300 mg, 0.50 mmol) and $Fe_2(CO)_9$ (250 mg, 0.68 mmol) were weighted in the glove-box in a Schlenk

tube, then toluene (15 ml) was added. The mixture was heated over night, at 70 °C, under magnetic stirring. The completeness of the reaction was checked by ^{31}P-NMR spectroscopy. After cooling down to r.t., the red solution was filtered through celite on a glass frit and then almost all the solvent was removed under vacuum. The remaining solution was deposited onto the top of a short silica-gel column eluted with toluene. An orange fraction was recuperated and after removing the solvent on a rota-evaporator, precipitation with pentane and drying under vacuum, a red solid was recovered. Recrystallization in hexane yielded bright red crystals of complex (200 mg, 54%). Anal. Calc. for $C_{35}H_{26}O_3P_2S_4Fe\cdot(C_6H_{14})_{1/4}$: C, 57.52; H, 3.90. Found: C, 57.61; H, 3.95%. IR (KBr, cm^{-1}): ν_{CO} 1901, 1925, 1991. ^{31}P-NMR (C_6D_6): δ 86.7. ^{1}H-NMR (C_6D_6): δ 1.24 (s, 6H, CH_3), 7.02 (bs, 12H, H_{meta}, H_{para}), 7.74 (bs, 8H, H_{ortho}). ^{13}C-NMR (C_6D_6): δ 13.2 (s, CH_3), 114.2 (s, $S_2C{=}CS_2$), 114.4 (s, $S_2C{=}CS_2$), 123.0 (s, $CH_3C{=}$), 129.0 (vt, X part of an ABX system, $\Sigma J_{CP} = 10.2$ Hz, C_{meta}), 130.8 (s, C_{para}), 132.8 (vt, X part of an ABX system, $\Sigma J_{CP} = 11.5$ Hz, C_{ortho}), 135.4 (vt, X part of an ABX system, $\Sigma J_{CP} = 46.8$ Hz, C_{ipso}), 151.9 (vt, X part of an ABX system, $\Sigma J_{CP} = 77.6$ Hz, PC=CP), 219.3 (t, $^2J_{CP} = 6.6$ Hz, CO). EIMS; m/z (ion, rel. intensity): 740 (M, 1), 712 (M − CO, 11), 684 (M − 2CO, 27), 656 (M − 3CO, 93), 600 (M − $Fe(CO)_3$, 44).

*4.2.8. [Tetrakis(diphenylphosphino)tetrathiafulvalene]-bis[tricarbonyl(iron)], [**P4**][Fe(CO)$_3$]$_2$*

To a mixture of **P4** (300 mg, 0.32 mmol) and $Fe_2(CO)_9$ (300 mg, 0.82 mmol), weighted in the glove-box in a Schlenk tube, toluene (20 ml) was added. The resulting suspension is stirred over night at 70 °C. After this period the reaction was complete and the deep red solution was filtered over celite. Chromatographic separation through a short silica-gel column eluted with toluene, followed by evaporation of solvent under vacuum and precipitation with pentane allowed the obtention of the complex as an orange solid (220 mg, 56%). Suitable crystals for X-ray analysis have been obtained by recrystallization in acetonitrile or in toluene. In the second case the crystals contain toluene. Anal. Calc. for $C_{60}H_{40}O_6P_4S_4Fe_2\cdot(C_7H_8)_3$: C, 64.98; H, 4.31. Found: C, 64.94; H, 4.34%. IR (KBr, cm^{-1}): ν_{CO} 1905, 1923, 1987. ^{31}P-NMR (C_6D_6): δ 87.2. ^{1}H-NMR (C_6D_6): δ 7.04 (bs, 24H, H_{meta}, H_{para}), 7.76 (bs, 16H, H_{ortho}). ^{13}C-NMR (CD_2Cl_2): δ 119.1 (s, $S_2C{=}CS_2$), 129.0 (vt, X part of an ABX system, $\Sigma J_{CP} = 10.3$ Hz, C_{meta}), 131.1 (s, C_{para}), 132.5 (vt, X part of an ABX system, $\Sigma J_{CP} = 11.6$ Hz, C_{ortho}), 134.5 (vt, X part of an ABX system, $\Sigma J_{CP} = 47.0$ Hz, C_{ipso}), 151.2 (vt, X part of an ABX system, $\Sigma J_{CP} = 77.5$ Hz, PC=CP), 218.9 (t, $^2J_{CP} = 6.8$ Hz, CO). EIMS; m/z (ion, rel. intensity): 600 (M − $2Fe(CO)_3 - PPh_2 - 2Ph$, 44).

Table 6
Crystallographic data

	[**P4**][W(CO)$_4$]$_2$	[**P2**][Re(CO)$_3$Cl]	[**P2**][Fe(CO)$_3$]	[**P4**][Fe(CO)$_3$]$_2$
Empirical formula	$C_{83}H_{64}O_8P_4S_4W_2$	$C_{42}H_{34}ClO_3P_2ReS_4$	$C_{36.5}H_{29.5}O_3P_2S_4Fe$	$C_{60}H_{40}O_6P_4S_4Fe_2$
Formula mass	1809.16	998.52	762.13	1220.74
Crystal dimensions (mm)	$0.51\times0.06\times0.06$	$0.36\times0.06\times0.03$	$0.30\times0.15\times0.10$	$0.58\times0.20\times0.04$
Crystal system	Monoclinic	Orthorhombic	Orthorhombic	Triclinic
Space group	$P2_1/c$	$Pna2_1$	$Pbca$	$P\bar{1}$
Temperature (K)	150	293	293	250
Unit cell dimensions				
a (Å)	11.7651(8)	37.4504(18)	19.653(4)	8.6014(17)
b (Å)	19.4854(11)	11.2345(5)	21.216(4)	11.491(2)
c (Å)	16.9667(12)	20.3263(9)	34.820(7)	15.417(3)
α (°)	90.	90.	90.	77.93(3)
β (°)	106.377(8)	90.	90.	86.00(3)
γ (°)	90.	90.	90.	71.07(3)
V (Å^3)	3731.8(4)	8552.0(7)	14519(5)	1409.5(5)
Z	2	8	16	1
D_{calc} (g cm^{-3})	1.610	1.551	1.395	1.438
μ (mm^{-1})	3.335	3.211	0.768	0.827
Data collected	28 992	47 739	86 225	5096
Independent data	7204	16 263	14 150	5096
R_{int}	0.0428	0.1589	0.1452	0.0570
Observed data	5682	8031	5443	3168
Parameters refined	470	857	838	343
$R(F)$	0.0219	0.0578	0.0456	0.0348
$wR(F^2)$	0.0416	0.0972	0.0857	0.0543
Goodness-of-fit (obs.)	0.876	0.807	0.751	0.728
Residual d (e Å^{-3})	0.54 and −0.73	1.34 and −0.78	0.245 and −0.194	0.289 and −0.278

4.3. Crystallography

Data were collected on a Stoe IPDS diffraction system at r.t. unless otherwise specified. Details about data collection and solution refinement are given in Table 6. Structures were solved by direct methods (SHELXS) and refined by full-matrix least-squares procedures. All atoms were refined anisotropically except those of the disordered toluene molecules found in the structures of **[P4]**$[W(CO)_4]_2$[toluene]$_3$ and **[P2]**$[Re(CO)_3Cl]$[toluene]. Hydrogen atoms were introduced at calculated positions (except on the disordered toluene molecules) introduced in structure factor calculations and not refined (riding model).

5. Supplementary material

Crystallographic data for the structural analysis have been deposited with the Cambridge Crystallographic Data Centre, CCDC nos. 166271–166274 for compounds **P4**$[W(CO)_4]_2$, **P2**$Re(CO)_3Cl$, **P4**$[Fe(CO)_3]_2$, and **P2**$Fe(CO)_3$, respectively. Copies of this information may be obtained free of charge from The Director, CCDC, 12 Union Road, Cambridge CB2 1EZ, UK (Fax: +44-1223-336033; e-mail: deposit@ccdc.cam.ac.uk or www: http://www.ccdc.cam.ac.uk).

References

[1] (a) P.F. Crossing, M.R. Snow, J. Chem. Soc. A (1971) 610;
(b) L.F. Warren, M.A. Bennet, Inorg. Chem. 15 (1976) 3126;
(c) F.L. Wimmer, M.R. Snow, A.M. Bond, Inorg. Chem. 13 (1974) 1617.
[2] (a) A.M. Bond, R. Colton, J.J. Jackowski, Inorg. Chem. 14 (1975) 274 (see also p. 2526);
(b) A.M. Bond, R. Colton, F. Daniels, D.R. Fernando, F. Marken, Y. Nagaosa, R.F.M. Van Steveninck, J.N. Walter, J. Am. Chem. Soc. 115 (1993) 9556.
[3] (a) J.C. Kotz, C.L. Nivert, J. Organomet. Chem. 52 (1973) 387;
(b) J.C. Kotz, C.L. Nivert, J.M. Lieber, R.C. Reed, J. Organomet. Chem. 91 (1975) 87.
[4] (a) M. Fourmigué, P. Batail, J. Chem. Soc. Chem. Commun. (1991) 1370;
(b) M. Fourmigué, Y.-S. Huang, Organometallics 12 (1993) 797;
(c) F. Gerson, A. Lamprecht, M. Fourmigué, J. Chem. Soc. Perkin Trans. 2 (1996) 1409.
[5] M. Fourmigué, P. Batail, Bull. Soc. Chim. Fr. 129 (1992) 29.
[6] M. Fourmigué, C.E. Uzelmeier, K. Boubekeur, S.L. Bartley, K.R. Dunbar, J. Organomet. Chem. 529 (1997) 343.
[7] P. Pellon, E. Brule, N. Bellec, K. Chamontin, D. Lorcy, J. Chem. Soc. Perkin Trans. 1 (2000) 4409.
[8] J. Chatt, H.R. Watson, J. Chem. Soc. London (1961) 4980.
[9] P.E. Garrou, Inorg. Chem. 14 (1975) 1435.
[10] (a) A.M. Bond, R. Colton, M.E. McDonald, Inorg. Chem. 17 (1978) 2842;
(b) P.J. Giordano, M.S. Wrighton, J. Am. Chem. Soc. 101 (1979) 2888.
[11] (a) R.S. Berry, J. Chem. Phys. 32 (1960) 933;
(b) I. Ugi, D. Marquarding, H. Klusacek, P. Gillespie, F. Ramirez, Acc. Chem. Res. 4 (1971) 288;
(c) F.A. Cotton, K.I. Hardcastle, G.A. Rusholme, J. Coord. Chem. 2 (1973) 217.
[12] G.R. Langford, M. Akhtar, P.D. Ellis, A.G. MacDiarmid, J.D. Odom, Inorg. Chem. 14 (1975) 2937.
[13] G. Hogarth, T. Norman, Inorg. Chim. Acta 248 (1996) 167.
[14] C.-H. Ueng, L.-C. Leu, Acta Crystallogr. C 47 (1991) 725.
[15] K. Maitra, V.J. Catalano, J.H. Nelson, J. Organomet. Chem. 529 (1997) 409.
[16] T.M. Miller, K.J. Ahmed, M.S. Wrighton, Inorg. Chem. 28 (1989) 2347.
[17] C.E. Uzelmeier, S.L. Bartley, M. Fourmigué, R. Rogers, G. Grandinetti, K.R. Dunbar, Inorg. Chem. 37 (1998) 6706.
[18] (a) F.W.B. Einstein, C.-H. Huang, Acta Crystallogr. B 34 (1978) 1486;
(b) L.P. Battaglia, D. Delledonne, M. Nardelli, C. Pelizzi, G. Predieri, G.P. Chiusoli, J. Organomet. Chem. 330 (1987) 101;
(c) L.-S. Luh, L.-K. Liu, Inorg. Chim. Acta 206 (1993) 89.
[19] (a) A.W. Addition, R.T. Nageswara, J. Reedjik, J. van Rijn, G.C. Verschoor, J. Chem. Soc. Dalton Trans. (1984) 1349;
(b) D.K. Mills, Y.M. Hsiao, P.J. Farmer, E.V. Atnip, J.H. Reibenspies, M.Y. Darensbourg, J. Am. Chem. Soc. 113 (1991) 1421.
[20] G. Hogarth, J. Organomet. Chem. 406 (1991) 391.
[21] A.M. Bond, D.J. Darensbourg, E. Moccelin, B.J. Stewart, J. Am. Chem. Soc. 103 (1981) 6827.
[22] P.K. Baker, N.G. Connelly, B.M.R. Jones, J.P. Maher, K.R. Somers, J. Chem. Soc. Dalton Trans. (1980) 579.
[23] J.H. MacNeil, A.C. Chiverton, S. Fortier, M.C. Baird, R.C. Hynes, A.J. Williams, K.F. Preston, T. Ziegler, J. Am. Chem. Soc. 113 (1991) 9834.
[24] D.J. Darensbourg, M.A. Murphy, J. Am. Chem. Soc. 100 (1978) 463.